

Sulforaphene inhibits triple negative breast cancer through activating tumor suppressor *Egr1*

Ming Yang¹ · Wendi Teng¹ · Yue Qu¹ · Haiyong Wang¹ · Qipeng Yuan¹

Received: 26 February 2016 / Accepted: 25 June 2016 / Published online: 4 July 2016
© Springer Science+Business Media New York 2016

Abstract Sulforaphene (SFE, 4-methylsulfinyl-3-butenyl isothiocyanate) is a member of isothiocyanates, which is derived from radish seeds. It has shown that multiple isothiocyanates, such as sulforaphane, can effectively inhibit cancer cell proliferation in vitro and in vivo. However, it is still largely unknown if SFE could impact breast cancer. In this study, we investigated the anticancer effects of SFE on triple negative breast cancer (TNBC) via a series of in vitro and in vivo assays. We found that SFE can significantly inhibit cell proliferation in multiple TNBC cell lines through inducing G2/M phase arrest as well as cell apoptosis. Nude mice xenograft assays support the anti-TNBC role of SFE in vivo. Interestingly, SFE can repress expression of cyclinB1, Cdc2, and phosphorylated Cdc2, and, then, induced G2/M phase arrest of TNBC cells. To identify SFE target genes, we detected genome-wide gene expression changes through gene expression profiling and observed 27 upregulated and 18 downregulated genes in MDA-MB-453 cells treated with SFE. Among these genes, *Egr1* was successfully validated as a consistently activated gene after SFE treatment in TNBC MDA-MB-453 and MDA-MB-436 cells. *Egr1* overexpression inhibited proliferation of TNBC cells. However, *Egr1* knock-down using siRNAs significantly promoted TNBC cell

growth, indicating the tumor suppressor nature of *Egr1*. In sum, we for the first time found that SFE might be a potential anti-TNBC natural compound and its antiproliferation effects might be mediated by tumor suppressor *Egr1*.

Keywords Sulforaphene · Triple Negative Breast Cancer · Isothiocyanate · *Egr1*

Introduction

Breast cancer is one of the most common cancers in the world. In the United States, it is estimated that there were about 230,000 breast cancer patients with invasive diseases with more than 40,000 deaths in 2015 [1, 2]. Although the number of breast cancer deaths has fallen over the past 15 years, it remains the most common serious threat to human health and the second leading cause of cancer deaths among women. Triple negative breast cancer (TNBC) is a pathological subtype of breast cancer and is characterized by the absence of the estrogen receptor (ER), progesterone receptor (PR), and human epidermal growth factor receptor 2 (HER2) [3]. Approximately 15–20 % of the globally diagnosed breast cancers are designated ER–, PR– and HER2– negative [4]. Among the deadliest aspects of TNBC cells are their aggressive nature and high metastatic ability, which thereby render them resistant to most commonly available therapies [5]. No specific molecular targets for this subgroup of breast cancer patients are yet identified, thus providing a major arena for exploration [6]. Therefore, development of therapeutic strategies to target the TNBC cells may help to improve TNBC treatment.

Ming Yang, Wendi Teng and Yue Qu have contributed equally to this work.

✉ Qipeng Yuan
yuanqp@mail.buct.edu.cn

¹ State Key Laboratory of Chemical Resource Engineering, Beijing Laboratory of Biomedical Materials, College of Life Science and Technology, Beijing University of Chemical Technology, P. O. Box 75, 100029 Beijing, China

In the past few years, a number of new drug approvals and the presentation of results from large, randomized studies that have changed treatment algorithms offer hope of substantial improvements in outcomes in both early-stage and advanced breast cancer [7]. Accumulated epidemiologic studies reported that 67 % of 87 case–control studies found an inverse association between some type of cruciferous vegetable intake and cancer risk [8]. Sulforaphane (SFE, 4-methylsulfinyl-3-butenyl isothiocyanate), a member of isothiocyanate family derived from radish [9], has shown a great potential as an anticancer agent [10–12]. Several recent case–control studies in the US, Sweden, and China found that measures of cruciferous vegetable intake were significantly lower in women diagnosed with breast cancer than in cancer-free control groups [13–15].

In the current study, we identified a natural compound, SFE that exhibited substantial anticancer effects to different TNBC cell lines in vitro and in vivo. The antineoplastic activities of SFE may be mediated through an *Egr1*-dependent mechanism.

Materials and methods

Drugs, siRNAs, and plasmids

SFE (purity >95 %) was prepared and purified from radish seeds in our laboratory by preparative high-performance liquid chromatography (HPLC). The purity and chemical structure were identified by analytical HPLC, ESI–MS, and NMR [9]. SFE was resuspended in dimethyl sulfoxide (DMSO) for the following studies. Three *Egr1* siRNAs were used in the study, sequence1: 5'-GCCUAGUGAG CAUGACCAATT-3'; sequence2, 5'-CCAUGGACAACU ACCCUAATT-3'; sequence3, 5'-UCCCAGGACAAUUG AAAUUTT-3') (Life Technologies). The coding sequence of *Egr1* was cloned into pcDNA3.1(+) expression vector, and the sequence was verified by Sanger sequencing.

Cell lines and cell cultures

MDA-MB-231 was cultured in Dulbecco's modified Eagle (DMEM) medium with 10 % fetal bovine serum (FBS). MDA-MB-436 and MDA-MB-468 cells were cultured in complete RPMI 1640 medium with 10 % FBS, 100 mg/mL penicillin and 100 mg/mL streptomycin. Cells were maintained at 37 °C and 5 % CO₂. MDA-MB-453 was cultured in Leibovitz's L15 medium and maintained at 37 °C, but not CO₂. All the cell lines were purchased from the National Platform of Experimental Cell Resource for Sci-Tech (<http://cellresource.cn/>) (Beijing, China).

Proliferation assays

Cells were seeded in 96-well plates at an initial density of 2×10^5 per well. At each time point, cells were stained with 100 μ L of sterile MTT (0.5 mg/mL; Sigma) for 2 h at 37 °C, followed by removal of the culture medium and addition of 100 μ L of DMSO [16, 17]. Absorbance was measured at 490 nm. All experiments were done in triplicates.

Analysis of cell cycle and apoptosis

Cells were plated in 6-well plates and cultured overnight. The cells were treated with SFE for 24, 48, and 72 h. Cell apoptosis was determined using the Alexa Fluor[®] 488 annexin V/Dead Cell Apoptosis Kit (Catalog No. V13245; Invitrogen) using the FACSCalibur flow cytometer (FCM) (BD Biosciences), according to the manufacturer's instructions. For DNA content determination, TNBC cells were harvested after SFE treatment and washed twice with cooled PBS containing 10 % FBS, then suspended with PBS containing 3 % FBS and 70 % ethanol. Cells were treated with 1 mg/mL RNase A and stained with 5 mg/mL propidium iodide (Sigma). The analysis was performed by FCM to determine the percentage of cells with 2N DNA, at S phase, and with 4 N DNA content [18–21].

Microarray experiments

Affymetrix HTA2.0 microarrays were used. Data were converted to expression measures using the MAS5.0 algorithm (GeneChip operating software version 1.1) and raw data were imported into the GeneSpring data analysis program version 6.1 (Silicon Genetics, Palo Alto, CA, USA). Parameters used for bioinformatic analyses are described in details by Kennedy et al.

Real-time qPCR

Total cellular RNAs were extracted from MDA-MB-453 and MDA-MB-436 cells. After the reverse transcription of total RNA, qPCR was performed in triplicates using the QuantiFast SYBR Green PCR Kit (Qiagen, Valencia, CA) according to the manufacturer's instructions. Gene-specific primers for the selected genes were as follows: *Egr1*: forward: 5'-TACGAGCACCTGACCGCAGAGTC, reverse: 5'-AGGCTCCAGGGAAAAGCGGC-3'; *NQO1*: forward: 5'-GGCAGAAGAGCACTGATCGTA-3', reverse: 5'-TGA TGGGATTGAAGTTCATGGC-3'; *SCD*: forward: 5'-GGA GCCACCGCTCTTACAAA-3', reverse: 5'-ACGAGCCCA TTCATAGACATCA-3'; *GLCM*: forward: 5'-AATCAGC CCTGATTTGGTCAGG-3', reverse: 5'-CCAGCTGTGCA ACTCCAAGGAC-3'; *G6PD*: forward: 5'-TGAGCCAGA

TAGGCTGGAA-3', reverse: 5'-TAACGCAGGCGATGT
TGTC-3'; *NDRG1*: forward: 5'-GCCGCCTCCAAGATCT
CA-3', reverse: 5'-ACGTTACTCTGCATTTCTTCCTC-3';
IGFBP3: forward: 5'-CGCTACAAAGTTGACTACGAGT
C-3', reverse: 5'-GTCTTCCATTTCTCTACGGCAGG-3';
ID1: forward: 5'-CCAGAACCGCAAGGTGAG-3', reverse:
5'-GGTCCCTGATGTAGTCGATGA-3'.

Western blotting

Total proteins from various TNBC cells treated with vehicle control or SFE were extracted with radioimmuno-precipitation assay (RIPA) buffer [50 mmol/L Tris-HCl (pH 7.4), 150 mmol/L NaCl, 1 % NP40, 0.5 % sodium deoxycholate, 0.1 % SDS, 5 mmol/L EDTA]. Twenty micrograms of each protein extract were resolved on 10 % SDS-PAGE and transferred to Hybond-C nitrocellulose. The levels of *Egr1*, cyclinB1, Cdc2, and phosphorylated Cdc2 expression were determined by anti-*Egr1* (Santa Cruz), anti-cyclinB1 (Santa Cruz), anti-Cdc2 (Santa Cruz), anti-p-Cdc2 (Santa Cruz) antibodies. β -actin expression levels were measured using a monoclonal anti- β -actin (A 3853; Sigma) as a loading control.

In vivo tumor models

All animal experiments were conducted under the guidelines (HY-IACUC-10-048) [22]. To evaluate the anticancer effects of SFE in vivo, 6×10^6 MDA-MB-453 cells were implanted into the right breast fat pad of nude mice. The mice were monitored for tumor formation and growth. Mice were treated with 100 mg/kg SFE or solvent control via intravenous injection daily. Tumor weight was determined after sacrificing all mice.

Statistical analyses

To assess statistical significance, values were compared with controls with either Student's *t*-test or one-way ANOVA. An *P* value of less than 0.05 was used as the criterion of statistical significance, and all statistical tests were two-sided. All analyses were performed using SPSS software package (Version 16.0, SPSS Inc.).

Results

SFE inhibits proliferation of TNBC cells via inducing cell cycle arrest and apoptosis

To determine whether SFE could impact growth of TNBC in vitro, we treated the TNBC MDA-MB-436, MDA-MB-

453, MDA-MB-231, and MDA-MB-468 cells with various concentrations of SFE. The IC₅₀ values for 72 h of SFE treatment were 11.3 μ M for MDA-MB-436, 12.7 μ M for MDA-MB-453, 15.3 μ M for MDA-MB-231, and 20.7 μ M for MDA-MB-468 (Fig. 1a). The anti-TNBC effects of SFE were dose dependent, as increasing concentrations of SFE decreased the number of viable cells (Fig. 1b). In addition, the anti-TNBC effect of SFE was also time dependent (Fig. 1c). Therefore, we concluded that SFE was capable of inhibiting the proliferation of TNBC cells.

We next examined whether the inhibition of cell proliferation was due to alterations of cell cycle and/or apoptosis. It has been showed that SFE induced cell cycle arrest of MDA-MB-436 and MDA-MB-453 cells after 48 and 72 h of treatment. As shown in Fig. 1d, MDA-MB-436 and MDA-MB-453 cells were arrested at G₂/M phase after SFE treatment compared to DMSO treatment (*P* < 0.05). We also detected whether SFE could induce apoptosis of TNBC cells. Interestingly, it has been found that there were significantly increased apoptotic TNBC cells after SFE treatment (Fig. 1e). In detail, 15 μ M SFE can induce 14.57 or 20.36 % of apoptotic MDA-MB-436 or MDA-MB-453 cells (Fig. 1e). Taken together, SFE could inhibit cell proliferation by inducing cell cycle arrest as well as apoptosis.

Whole-genome expression profiling changes of TNBC cells after SFE treatment

We next evaluated the changes of the gene expression profile of MDA-MB-453 cells after SFE treatment. Both microarray files are available from the National Center for Biotechnology and the Institute of Gene Expression Omnibus (GEO) repository database (accession number GSE77566). The following criteria were used to determine differentially expressed genes (the SFE group vs. The DMSO group): upregulated genes, with fold changes ≥ 2 ; downregulated genes, with fold changes ≤ 0.5 . A total of 53 genes were identified (30 genes with increased expression and 23 genes with decreased expression (Fig. 2a, b).

After literature research of these 53 genes, we finally chose eight previously reported cancer-related genes to validate by real-time qPCR (*Egr1*, *NQO1*, *SL7A11*, *G6PD*, *GCLM*, *SCD*, *ID1*, and *IGFBP3*). As shown in Fig. 2c, there were 17.85, 15.32, 13.19, 7.15, or 2.1 folds of increased expression of *Egr1*, *NQO1*, *SL7A11*, *G6PD*, or *GCLM* genes in TNBC cells treated with SFE compared to DMSO, respectively. Among these genes, *Egr1* is the most simulated gene after SEF treatment. Moreover, we observed a 0.68, 0.29, or 0.48 folds of decreased expression of *SCD*, *ID1*, and *IGFBP3* genes in SFE-treated cells compared to DMSO (Fig. 2c).

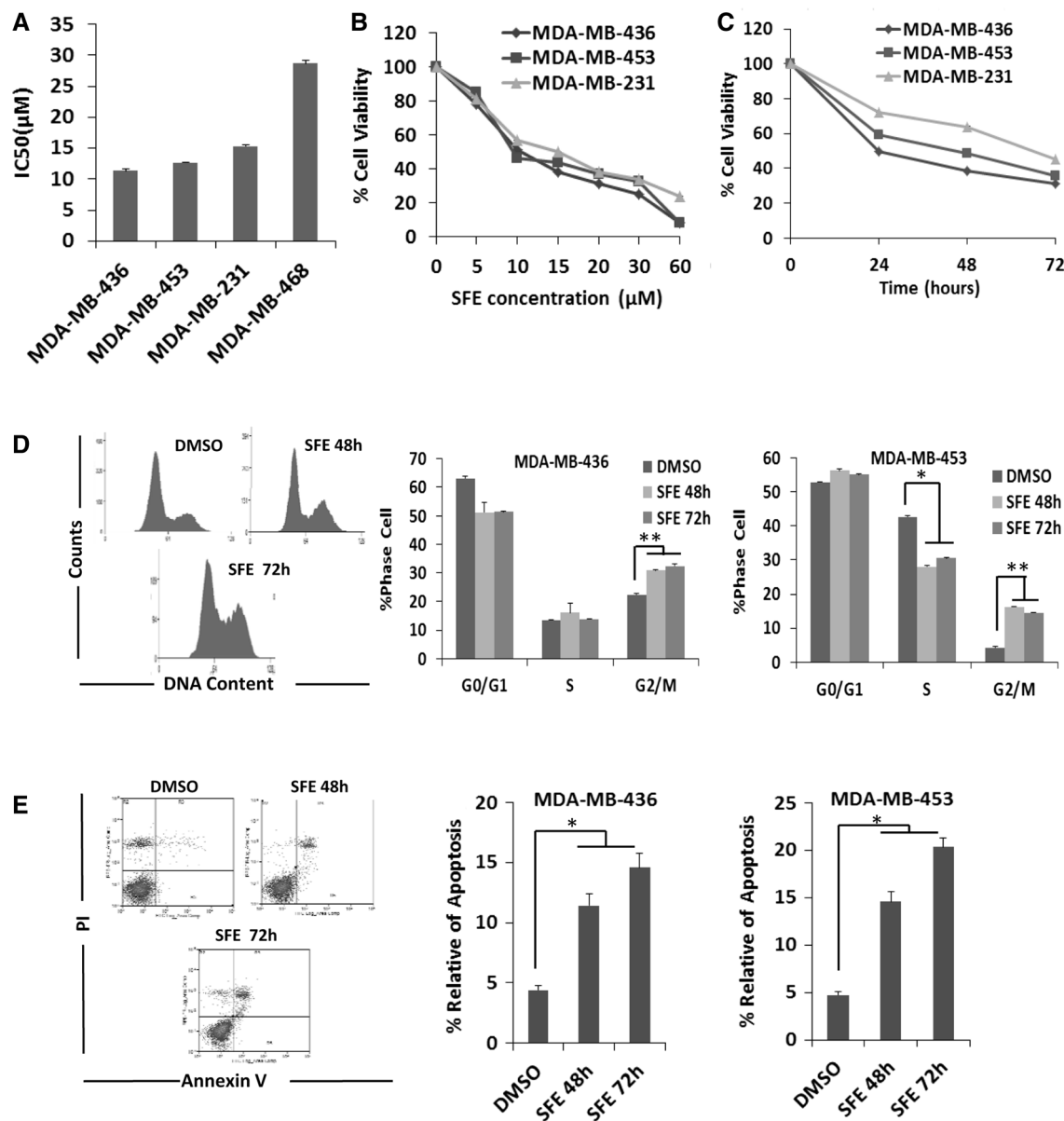


Fig. 1 SFE inhibits the proliferation of TNBC and induces cell cycle arrest and apoptosis. **a** The IC₅₀ values of MDA-MB-436, MDA-MB-453, MDA-MB-231, and MDA-MB-468 cells with various concentrations of SFE after 72 h of treatment. **b** MDA-MB-436, MDA-MB-453, MDA-MB-231 cells were treated with various concentrations of SFE for 72 h, and the inhibition of cell proliferation was determined through the MTT assays. **c** MDA-MB-436, MDA-MB-453, MDA-MB-231 cells were treated with 15 μ M SFE for 24, 48, and 72 h, and

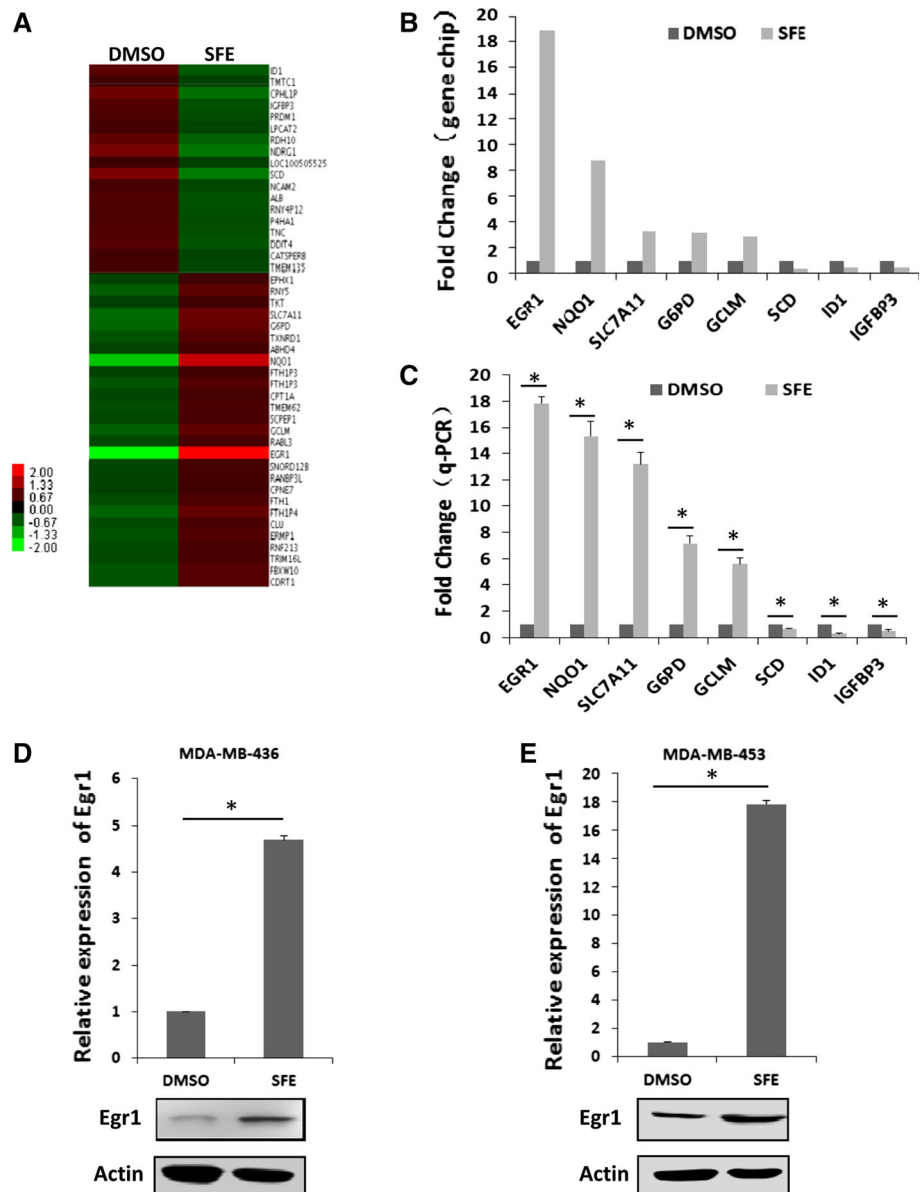
the inhibition of cell proliferation was determined through the MTT assays. **d** MDA-MB-436 and MDA-MB-453 cells were treated with 15 μ M SFE for 48 and 72 h. The cell cycle profiles are shown. The histogram of statistical analysis on the *right* is the percentage of all phase cells. **e** Apoptosis was analyzed by Annexin-V-PI staining using flow cytometry. The histogram of statistical analyses on the *right* is the percentage of cell death. DMSO, the negative control; * $P < 0.05$; ** $P < 0.01$

To confirm that the observed changes in mRNA expression reflected changes in protein expression, we detected the most upregulated gene, *Egr1* by western blots. Consistent with the qPCR results, the protein expression of *Egr1* was significantly increased in both MDA-MB-436 and MDA-MB-453 cells after treatment with SFE for 48 and 72 h (Fig. 2d, e). These results indicated that SFE induced *Egr1* expression in TNBC cells.

Egr1 as a potential SFE target in TNBC cells and inhibits TNBC proliferation

To investigating if *Egr1* acts as a potential target of SFE in TNBC, we transiently overexpressed *Egr1* in MDA-MB-436 and MDA-MB-453 cells. We found a significant inhibition of cell proliferation after *Egr1* overexpression in both TNBC cell lines (Fig. 3a, b). To

Fig. 2 Gene profiling and candidate gene validation. **a** The heatmap of a total of 53 differentially expressed genes after SFE treatment. **b** Candidate genes were examined by gene chip. **c** Candidate genes were validated using real-time qPCR. **d, e** Target gene was validated by real-time qPCR and western blot analyses in MDA-MB-436 and MDA-MB-453 cells



confirm the effects of *Egr1* on cell proliferation, we silenced *Egr1* expression in MDA-MB-436 and MDA-MB-453 cells with three different *Egr1* siRNAs (Fig. 3c, d). In line with the aforementioned results, knockdown of *Egr1* by siRNAs did significantly promote cell proliferation in both cell lines (all $P < 0.05$) (Fig. 3c, d).

To further explore the detailed mechanisms as to how *Egr1* impacts the proliferation of TNBC cells, we detected the changes of cell cycle profiles after SFE treatment and observed that it significantly increased the G₂/M phase fractions (both $P < 0.05$) (Fig. 4a). Additionally, the percentage of apoptotic TNBC cells was increased in *Egr1* overexpressed cells (Fig. 4b). These results were consistent

with the effects of SFE on TNMBC cells, indicating that *Egr1* is a key target of SFE in TNBC.

SFE-induced cell cycle arrest via the *Egr1*-cyclinB1-Cdc2 pathway

To examine the underline mechanisms of SFE-mediated cell cycle arrest in TNBC, we analyzed cyclinB1, Cdc2, phosphorylated-Cdc2 (p-Cdc2), and Cdc25c expression at different time points after SFE or DMSO treatment. In the SFE-treated MDA-MB-436 and MDA-MB-453 cells, the expression level of cyclinB1, Cdc2, p-Cdc2, and Cdc25c were markedly decreased in a time-dependent manner

Fig. 3 Effects of *Egr1* overexpression and knockdown on cell proliferation. Growth curve showing the growth of MDA-MB-436 and MDA-MB-453 cells in the presence of *Egr1* overexpression (a, b) and *Egr1* knockdown (c, d). The effects of *Egr1* overexpression (a, b) and *Egr1* knockdown (c, d) were analyzed by real-time qPCR in MDA-MB-436 and MDA-MB-453 cells. The effect of *Egr1* overexpression (a, b) and *Egr1* knockdown (c, d) was also analyzed by western blot analysis in MDA-MB-436 and MDA-MB-453 cells. *Scr* scrambled siRNAs. * $P < 0.05$; ** $P < 0.01$

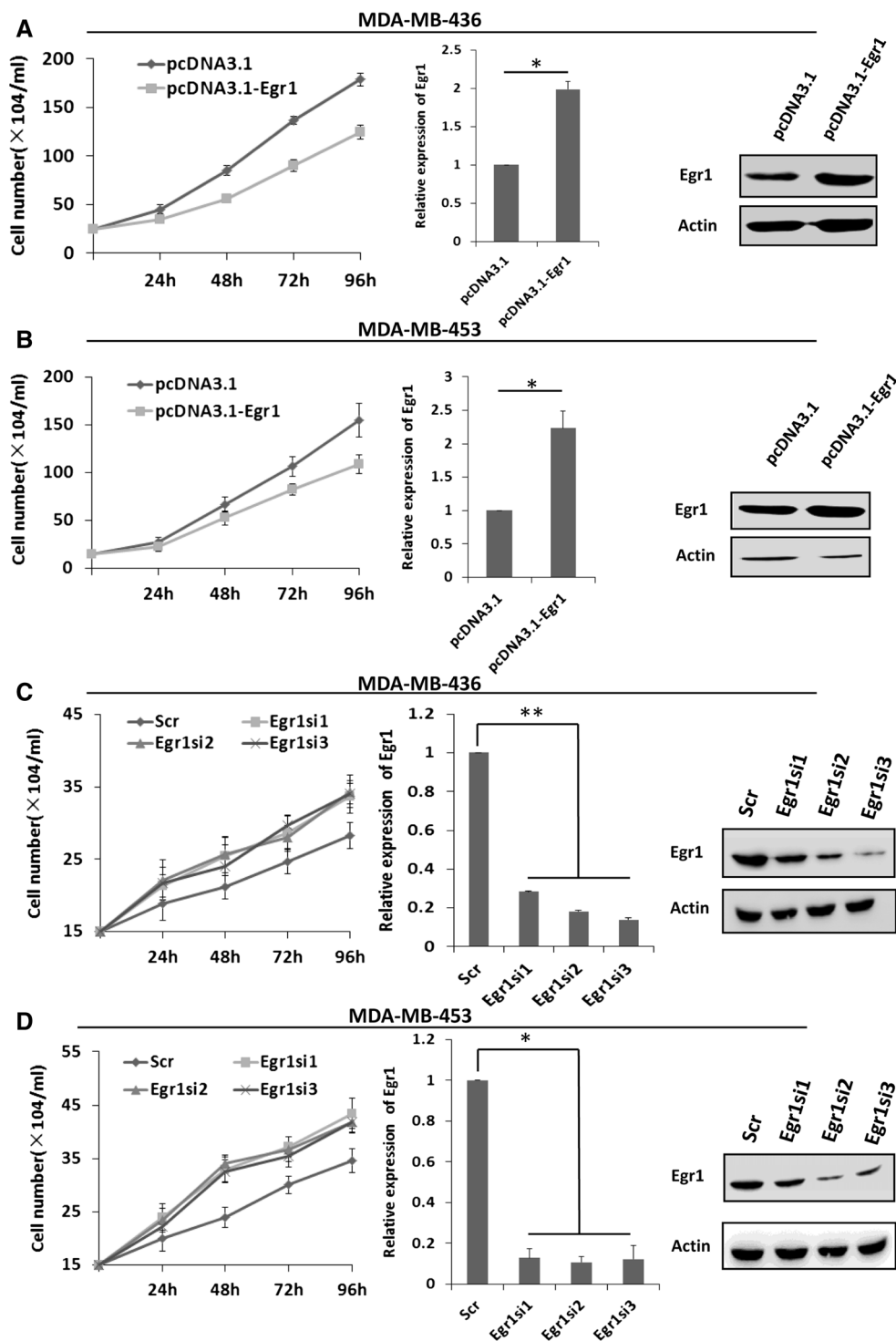
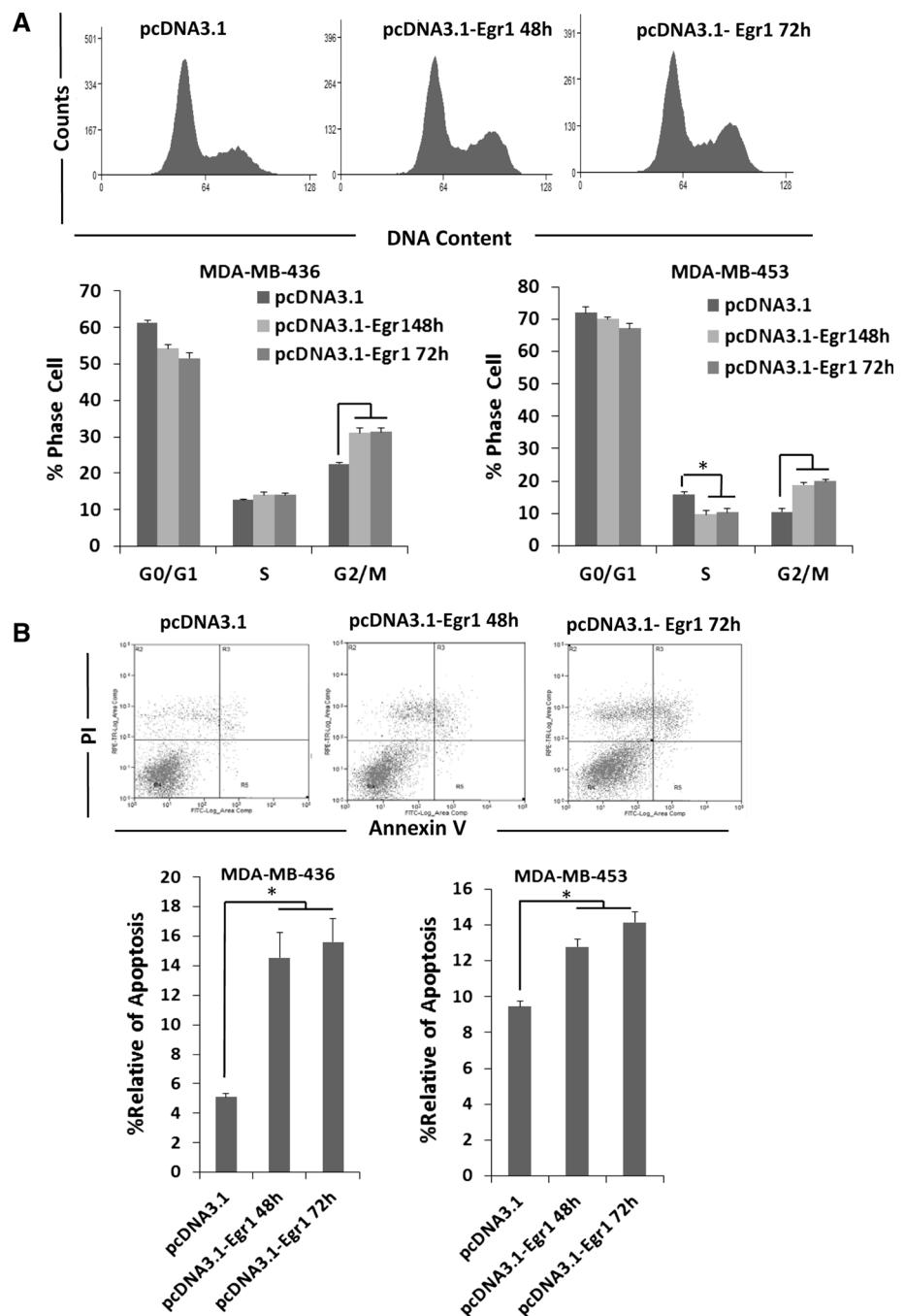


(Fig. 5a, b). This may partly explain why SFE could induce G₂/M arrest of TNBC cells. However, cyclinB1 did not show obvious changes after DMSO treatment at different time points. To examine if *Egr1* is involved in SFE-induced G₂/M phase arrest, we overexpressed *Egr1* and detected cyclinB1, Cdc2, p-Cdc2, and Cdc25c expression

in TNBC cells (Fig. 5c, d). The expression level of cyclinB1, Cdc2, p-Cdc2, and Cdc25c were significantly repressed after *Egr1* overexpression (Fig. 5c, d), which was consistent with SFE-induced gene expression changes, suggesting that SFE may induce cell cycle arrest via the EGR1-cyclinB1-Cdc2 pathway.

Fig. 4 Effects of *Egr1* overexpression and knockdown on cell cycle arrest and apoptosis. MDA-MB-436 and MDA-MB-453 cells were transfected with pcDNA3.1-*Egr1* for 48 or 72 h. **a** The cell cycle profiles. The histogram of statistical analyses on the right is the percentage of all phase cells. **b** Apoptosis was analyzed by Annexin-V-PI staining using flow cytometry. The histogram of statistical analyses on the right is the percentages of cell death. * $P < 0.05$; ** $P < 0.01$

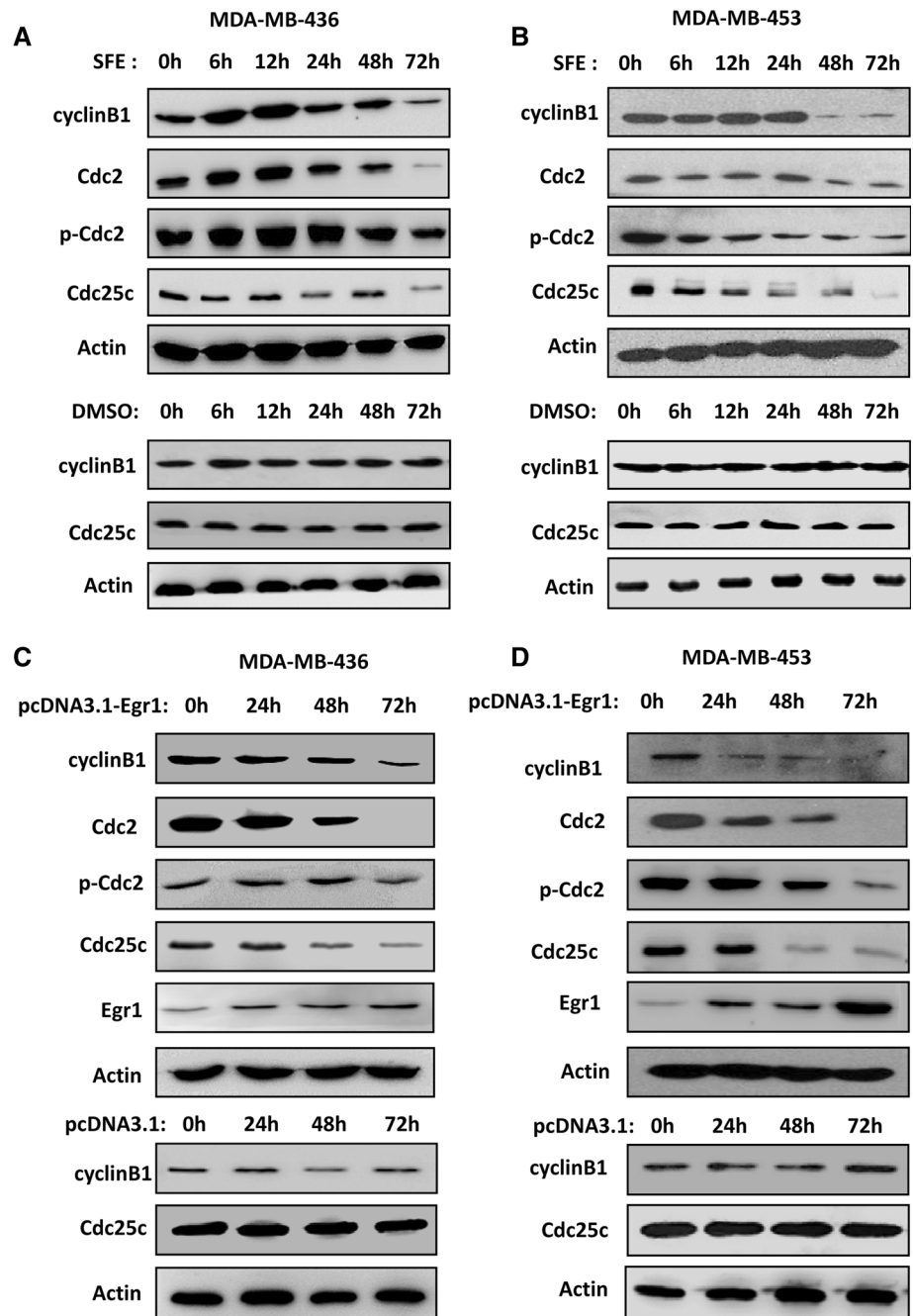


In vivo anti-TNBC effects of SFE

Nude mice xenografted with the MDA-MB-453 cells were used to test the SFE anticancer effects in vivo. As shown in Fig. 6a, SFE treatment did not impact mice body weights significantly. However, the tumors shrank obviously in mice that are given SFE compared to the controlled mice (Fig. 6b). After 15 days post SFE treatment, mice were sacrificed and tumors were isolated and

weighted (Fig. 6c, d). Significantly decreased tumor weights were observed (Fig. 6c). To confirm if *Egr1*, cyclinB1, and Cdc25c have similar expression changes as in the in vitro study, we examined their expressions in three pairs of TNBC xenografts (Fig. 6e). As anticipated, we observed significantly elevated expression of *Egr1* as well as reduced expressions of cyclinB1 and Cdc25c in xenografts of SFE-treated mice compared with those of DMSO-treated mice.

Fig. 5 Expression changes of the *Egr1*-cyclinB1-Cdc2 pathway. MDA-MB-436 (a) and MDA-MB-453 (b) cells were treated with 15 μ M SFE for 0, 6, 12, 24, 48, and 72 h. cyclinB1, Cdc2, and p-Cdc2 protein expression was analyzed by western blot. MDA-MB-436 (c) and MDA-MB-453 (d) cells were transfected with pcDNA3.1-*Egr1* for 24, 48, and 72 h. *Egr1*, cyclinB1, Cdc2, and p-Cdc2 protein expressions were examined



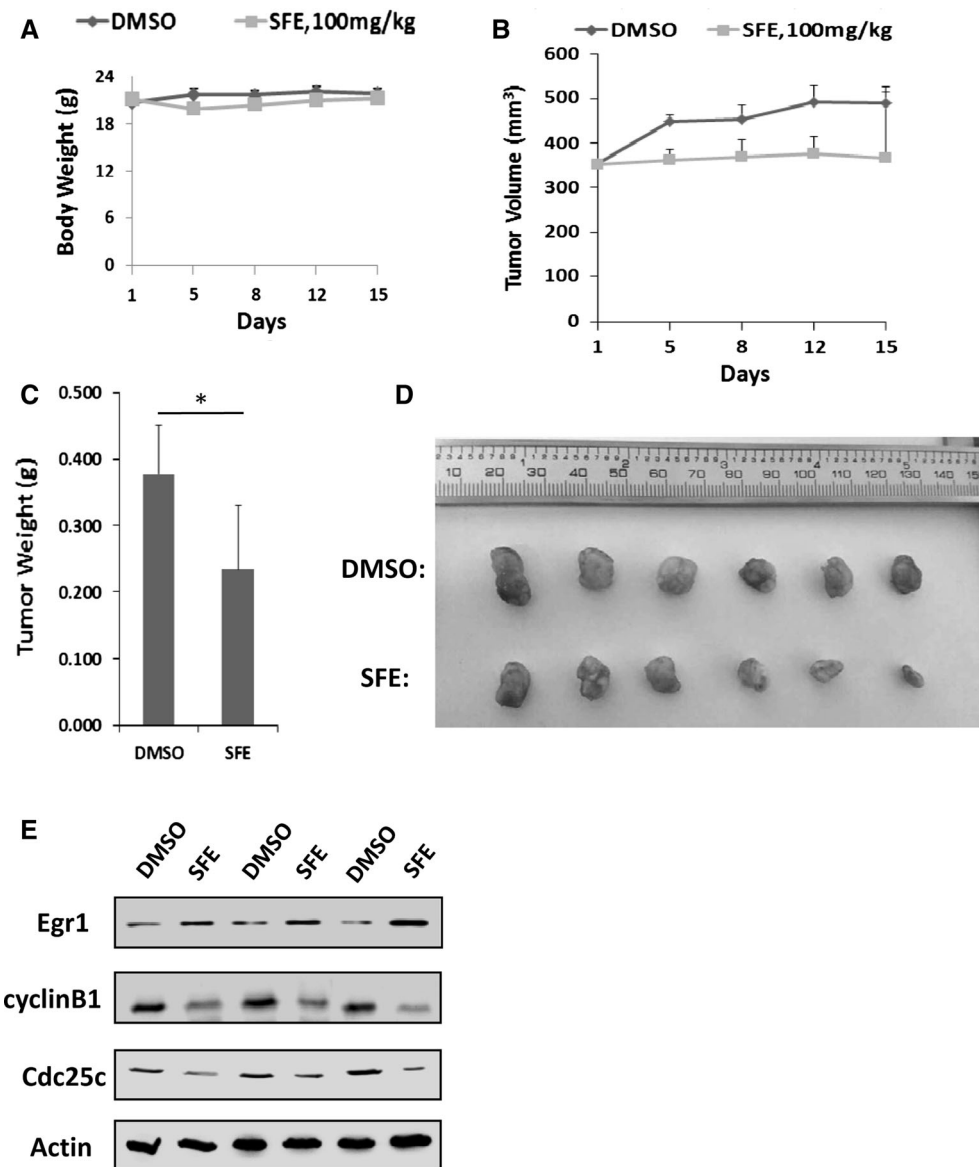
Discussion

SFE was a natural product purified from radish seeds that exerts antioxidant activities. In this study, we investigated the anti-TNBC activity of SFE in vitro and in vivo with a xenograft mouse model. It has been showed that SFE exhibited antiproliferative effects against multiple kinds of TNBC cells *ex vivo*. MDA-MB-468 is less sensitive to SFE than other cell lines, which may be due to homozygous deletion of PTEN in MDA-MB-468 cell (Basal A type TNBC). However, MDA-MB-231 has WT PI3 K. The

underline mechanism of SFE's anti-TNBC activities might be upregulating tumor suppressor *Egr1* and, then, inducing G2/M cell cycle arrest and apoptosis.

In eukaryotic cells, cyclins play a critical role in regulating cell cycle progression from the G2 through the M phase, including exit from the M phase. It has been shown that entry and exit from the M phase of the cell cycle are controlled by fluctuations in the activity of MPF, of which Cdc2 is the catalytic subunit and cyclin B1 is a regulatory element. Cyclin B1 accumulates during the S and G2 phases, and its induction and activation of MPF are

Fig. 6 In vivo effect of SFE on TNBC mouse model. **a** Mice body weights were measured every 3 days. **b** Tumor volumes were measured every 3 days. Tumor volume was calculated by the following formula: tumor volume (mm^3) = length (mm) \times width (mm) \times height (mm) \times 0.5. **c** Bar graph represented final tumor weight after SFE treatment. **d** The photograph showed each tumor after SFE treatment at 15 days



necessary to initiate the transition from the G₂ to the M phase. The cyclinB1/Cdc2 complex allows for the phosphorylation of Cdc2 at several sites, maintaining it in an inactive state and ensuring that mitosis does not occur prematurely [23–25]. This phosphorylation-regulated Cdc2 lose activity [26]. To gain further insight into the molecular mechanisms underlying SFE-induced cell cycle arrests of TNBC cells, we examined the levels of cyclinB1, Cdc2, and p-Cdc2. We found that cyclinB1, Cdc2, and p-Cdc2 were markedly decreased in a time-dependent manner. These results demonstrate that SFE induced G₂/M phase cell cycle arrest via the inhibition of cyclin B1, Cdc2, and p-Cdc2 expressions in TNBC cells.

The *Egr1* gene has been identified as an important mediator of activation and pathology of cancer cells

[27, 28]. *Egr1* is a transcription factor containing zinc finger DNA-binding motifs able to either activating or repressing gene transcription [29, 30]. As master switches controlling developmental processes, transcription factors are attractive candidates as intrinsic regulators of cellular fate including cell reprogramming. *Egr1* could modulate cellular phenotype through the regulation of over 300 target genes. In addition, *Egr1*-mediated transcription brings together a multitude of signaling cascades vital for cell growth, differentiation as well as apoptosis [30, 31]. Consistent with this context, we observed that *Egr1* may be a SFE target for TNBC cells.

In conclusion, we for the first time showed the anti-neoplastic effects of SFE, a potential small natural

compound, on TNBC cells. We also found that SFE could be therapeutically beneficial for TNBC through an *Egr1*-dependent mechanism.

Grant support This work was supported by the National High-Tech Research and Development Program of China (2015AA020950); the Fundamental Research Funds for the Central Universities (YS1407); the open project of State Key Laboratory of Molecular Oncology (SKL-KF-2015-05); Program for Changjiang Scholars and Innovative Research Team in University (IRT13045); Innovation and Promotion Project of Beijing University of Chemical Technology.

Compliance with ethical standards

Conflict of interest The authors declare no competing financial interests.

References

- Siegel RL, Miller KD, Jemal A (2015) Cancer statistics, 2015. *Cancer J Clin* 65:5–29
- Scalia-Wilbur J, Collins BL, Penson RT, Dizon DS (2016) Breast cancer risk assessment: moving beyond BRCA1 and 2. *Semin Radiat Oncol* 26:3–8
- Brenton JD, Carey LA, Ahmed AA, Caldas C (2005) Molecular classification and molecular forecasting of breast cancer: ready for clinical application. *J Clin Oncol* 23:7350–7360
- Jemal A, Bray F, Center MM, Ferlay J, Ward E, Forman D (2011) Global cancer statistics. *Cancer J Clin* 61:69–90
- Hsu YH, Yao J, Chan LC, Wu TJ, Hsu JL (2014) Definition of PKC- α , CDK6, and MET as therapeutic targets in triple-negative breast cancer. *Cancer Res* 74:4822–4835
- D'Amato NC, Rogers TJ, Gordon MA, Greene LI (2015) A TDO2-AhR signaling axis facilitates anoikis resistance and metastasis in triple-negative breast cancer. *Cancer Res* 75:4651–4664
- Witherby S, Rizack T, Sakr BJ, Legare RD, Sikov WM (2016) Advances in medical management of early stage and advanced breast cancer: 2015. *Semin Radiat Oncol* 26:59–70
- Verhoeven DT, Goldbohm RA, van Poppel G, Verhagen H, van den Brandt PA (1996) Epidemiological studies on brassica vegetables and cancer risk. *Cancer Epidemiol Biomark Prev* 5:733–748
- Kuang P, Song D, Yuan Q, Yi R, Lv X, Liang H (2013) Separation and purification of sulforaphane from radish seeds using macroporous resin and preparative high-performance liquid chromatography. *Food Chem* 136:342–347
- Pocasap P, Weerapreeyakul N, Barusrux S (2013) Cancer preventive effect of Thai rat-tailed radish (*Raphanus sativus* L. var. *caudatus* Alef). *J Funct Food* 5:1372–1381
- Papi A, Orlandi M, Bartolini G, Barillari J, Iori R, Paolini M, Ferroni F, Grazia Fumo M, Pedulli GF, Valgimigli L (2008) Cytotoxic and antioxidant activity of 4-methylthio-3-butenyl isothiocyanate from *Raphanus sativus* L. (Kaiware Daikon) sprouts. *J Agric Food Chem* 56:875–883
- Nastruzzi C, Cortesi R, Esposito E, Menegatti E, Leoni O, Iori R, Palmieri S (2000) In vitro antiproliferative activity of isothiocyanates and nitriles generated by myrosinase-mediated hydrolysis of glucosinolates from seeds of cruciferous vegetables. *J Agric Food Chem* 48:3572–3575
- Ambrosone CB, McCann SE, Freudenheim JL, Marshall JR, Zhang Y, Shields PG (2004) Breast cancer risk in premenopausal women is inversely associated with consumption of broccoli, a source of isothiocyanates, but is not modified by GST genotype. *J Nutr* 134:1134–1138
- Fowke JH, Chung FL, Jin F, Qi D, Cai Q, Conaway C, Cheng JR, Shu XO, Gao YT, Zheng W (2003) Urinary isothiocyanate levels, brassica, and human breast cancer. *Cancer Res* 63:3980–3986
- Terry P, Wolk A, Persson I, Magnusson C (2001) Brassica vegetables and breast cancer risk. *J Am Med Assoc* 285:2975–2977
- Zhao C, Yue B, Liu H, Sun C, Li W, Qu X (2012) SL-01, an oral gemcitabine derivative, inhibited human cancer growth more potently than gemcitabine. *Toxicol Appl Pharmacol* 262:293–300
- Bonnesen C, Eggleston IM, Hayes JD (2001) Dietary indoles and isothiocyanates that are generated from cruciferous vegetables can both stimulate apoptosis and confer protection against DNA damage in human colon cell lines. *Cancer Res* 61:6120–6130
- Choi S, Lew KL, Xiao H, Herman-Antosiewicz A (2007) D, L-Sulforaphane-induced cell death in human prostate cancer cells is regulated by inhibitor of apoptosis family proteins and Apaf-1. *Carcinogenesis* 28:151–162
- Gamet Payraastre L, Li P, Lumeau S, Cassar G, Dupont MA, Chevolleau S (2000) Sulforaphane, a naturally occurring isothiocyanate, induces cell cycle arrest and apoptosis in HT29 human colon cancer cells. *Cancer Res* 60:1426–1433
- Hu K, Qi YJ, Zhao J, Jiang HF, Chen X, Ren J (2013) Synthesis and biological evaluation of sulforaphane derivatives as potential antitumor agents. *Eur J Med Chem* 64:529–539
- Chang CC, Hung CM, Yang YR, Lee MJ, Hsu YC (2013) Sulforaphane induced cell cycle arrest in the G2/M phase via the blockade of cyclin B1/CDC2 in human ovarian cancer cells. *J Ovarian Res* 6:41
- Gould KA, Tochacek M, Schaffer BS, Reindl TM, Murrin CR, Lachel CM, VanderWoude EA, Pennington KL, Flood LA, Bynote KK et al (2004) Genetic determination of susceptibility to estrogen-induced mammary cancer in the ACI rat: mapping of Emca1 and Emca2 to chromosomes 5 and 18. *Genetics* 168:2113–2125
- Ruetz S, Fabbro D, Zimmermann J, Meyer T, Gray N (2003) Chemical and biological profile of dual Cdk1 and Cdk2 inhibitors. *Curr Med Chem Anti* 3:1–14
- Stark GR, Taylor WR (2006) Control of the G2/M transition. *Mol Biotechnol* 32:227–248
- Choi YH, Yoo YH (2012) Taxol-induced growth arrest and apoptosis is associated with the upregulation of the Cdk inhibitor, p21WAF1/CIP1, in human breast cancer cells. *Oncol Rep* 28:2163–2169
- Han SJ, Conti M (2006) New pathways from PKA to the Cdc2/cyclin B complex in oocytes: wee1B as a potential PKA substrate. *Cell Cycle* 5:227–231
- Milbrandt J (1987) A nerve growth factor-induced gene encodes a possible transcriptional regulatory factor. *Science* 238:797–799
- Bhattacharyya S, Fang F, Tourtellotte W, Varga J (2013) *Egr1*: new conductor for the tissue repair orchestra directs harmony (regeneration) or cacophony (fibrosis). *Am J Pathol* 229:286–297
- Rong Y, Hu F, Huang RP, Mackman N, Horowitz JM, Jensen RL et al (2006) Early growth response gene-1 regulates hypoxia-induced expression of tissue factor in glioblastoma multiforme through hypoxia-inducible factor-1 – independent mechanisms. *Cancer Res* 66:7067–7074
- Thiel G, Cibelli G (2002) Regulation of life and death by the zinc finger transcription factor *Egr1*. *J Cell Physiol* 193:287–292
- Redmond KL, Crawford NT, Farmer H, D'Costa ZC, O'Brien GJ, Buckley NE (2010) T-box 2 represses NDRG1 through an *Egr1*-dependent mechanism to drive the proliferation of breast cancer cells. *Oncogene* 29:3252–3262